

Inverses of Matérn Covariances on Grids

Joseph Guinness

Cornell University, Department of Statistics and Data Science

Abstract

We conduct a theoretical and numerical study of the aliased spectral densities and inverse operators of Matérn covariance functions on regular grids. We apply our results to provide clarity on the properties of a popular approximation based on stochastic partial differential equations; we find that it can approximate the aliased spectral density and the covariance operator well as the grid spacing goes to zero, but it does not provide increasingly accurate approximations to the inverse operator as the grid spacing goes to zero. If a sparse approximation to the inverse is desired, we suggest instead to select a KL-divergence-minimizing sparse approximation and demonstrate in simulations that these sparse approximations deliver accurate Matérn parameter estimates, while the SPDE approximation over-estimates spatial dependence.

1 Introduction

For two locations in \mathbb{R}^d separated by lag $h \in \mathbb{R}^d$, the Matérn covariance function is

$$M[h : \nu, d] = \frac{\sigma^2}{2^{\nu-1}\Gamma(\nu)} (\alpha\|h\|)^\nu K_\nu(\alpha\|h\|), \quad (1)$$

where $\sigma^2, \nu, \alpha > 0$, and K_ν is the modified Bessel function of the second kind. Guttorp and Gneiting (2006) provide a summary of its important properties and a detailed discussion of the history of the covariance function. This article presents a theoretical and numerical study of properties of the spectral density of the Matérn covariance when aliased to regular grids in one and two dimensions. The study of square root, inverse, and inverse square root operators follow naturally from an understanding of the aliased spectral density. These connections are reviewed in Section 2, with a more detailed treatment of the basic results given in Appendix A. These two sections can provide a refresher for most readers on these important topics.

The exponential covariance is a special case of the Matérn, arising when $\nu = 1/2$. Due to the fact that an autoregressive model of order 1 has exactly an exponential covariance, the inverse of an exponential covariance matrix is exactly sparse when the dimension of the domain is 1, meaning that many of the entries of the inverse matrix are exactly equal to zero. In fact, the exact sparsity holds even when the observation locations do not form a regular grid. To our knowledge, there are no other exact sparsity results for the inverse of Matérn covariance matrices. Lindgren et al. (2011) proposed that the inverse of Matérn covariance matrices can be approximated by sparse matrices when $\nu + d/2$ is an integer. This approximation is commonly referred to as the stochastic partial differential equation (SPDE) approximation and builds on work by Whittle (1954), Whittle (1963), and Besag (1981). We

investigate this sparsity claim and find that there is nothing particularly special with regards to sparsity about the $\nu = 3/2$, $d = 1$ case or the $\nu = 1$, $d = 2$ case, relative to other values of ν . Further, by studying the spectral densities implied by the SPDE approximation, we show that the SPDE over-approximates power at the highest frequencies by at least a factor of 2 in the $d = 1$, $\nu = 3/2$ case and by as much as a factor of 2.7 in the $d = 2$, $\nu = 1$ case. This result suggests an explanation for why Guinness (2018) found that SPDE approximations were less accurate than Vecchia’s approximation (Vecchia, 1988).

We show in numerical studies that the increase in power at the highest frequencies impacts the accuracy of the SPDE approximation to the inverse covariance operator, and our simulation study shows that this leads to over-estimation of spatial ranges. The over-estimation was a feature discussed by Lee and Kaufman in the original SPDE paper (Lindgren et al., 2011, p. 479), with the discussion centered on boundary effects. Though boundary effects are important when working with approximations to the inverse covariance matrix, the present paper suggests instead that the over-estimation stems from the fact that the SPDE approximation has too much power at the highest frequencies, causing the likelihood to select a larger range parameter in order to compensate. When a sparse approximation to the inverse of a covariance matrix on a grid is desired, we propose instead to choose the entries of the inverse to minimize the KL-divergence to the targeted model. On regular grids with periodic boundary conditions, the KL-divergence can be computed quickly via the spectral densities.

Section 2 contains a general background on spectral theory for stationary random fields on grids. Section 3 provides a theoretical study of spectral properties of Matérn covariances in particular, and of SPDE approximations to them. Section 4 details specific computational procedures used to evaluate the spectral densities and the inverse operators. Section 5 contains numerical studies and a simulation study, and Section 6 concludes with a discussion.

2 Background

The details for all derivations in this section are spelled out in Appendix A. Let $Y : \mathbb{R}^d \rightarrow \mathbb{R}$ be a stationary process with autocovariance function $A[h] = \text{Cov}(Y[x+h], Y[x])$. Due to Bochner’s theorem (cf. Stein, 1999), $A[\cdot]$ is positive definite when

$$A(\omega) := \int_{\mathbb{R}^d} A[h] \exp(-i2\pi\omega \cdot h) dh > 0 \quad \text{for all } \omega \in \mathbb{R}^d. \quad (2)$$

The covariance function can be recovered by inverting the Fourier transform,

$$A[h] = \int_{\mathbb{R}^d} A(\omega) \exp(i2\pi\omega \cdot h) d\omega. \quad (3)$$

We call $A(\cdot)$ the spectral density for $A[\cdot]$. Our notational convention uses the same letter for the spectral density and covariance function, and distinguishes the two with the type of bracket: round for spectral densities and square for covariances. For $\Delta > 0$, define the interval $\mathbb{T}_\Delta = [0, 1/\Delta]$ and hypercube \mathbb{T}_Δ^d . When $h \in \mathbb{Z}^d$, the inverse Fourier transform can be rewritten as

$$A[\Delta h] = \int_{\mathbb{T}_\Delta^d} \sum_{k \in \mathbb{Z}^d} A(\omega + k/\Delta) \exp(i2\pi\Delta\omega \cdot h) d\omega =: A_\Delta[h], \quad (4)$$

which uses the aliasing property of complex exponentials and introduces a notation $A_\Delta[\cdot] : \mathbb{Z}^d \rightarrow \mathbb{R}$ for covariances on a grid with spacing Δ . We define

$$A_\Delta(\omega) = \sum_{k \in \mathbb{Z}^d} A(\omega + k/\Delta) \quad (5)$$

to be the aliased spectral density for A on a grid with spacing Δ . The discrete covariances and the aliased spectral density are related via

$$A_\Delta[h] = \int_{\mathbb{T}_\Delta^d} A_\Delta(\omega) \exp(i2\pi\Delta\omega \cdot h) d\omega, \quad (6)$$

$$A_\Delta(\omega) = \Delta^d \sum_{h \in \mathbb{Z}^d} A_\Delta[h] \exp(-i2\pi\Delta\omega \cdot h), \quad (7)$$

so that $A_\Delta[\cdot]$ is the integral Fourier transform of $A_\Delta(\cdot)$ over \mathbb{T}_Δ^d , and $A_\Delta(\cdot)$ is the infinite discrete Fourier transform of $A_\Delta[\cdot]$.

We say that A_Δ^{-1} is the inverse of A_Δ if

$$\Delta^d \sum_{k \in \mathbb{Z}^d} A_\Delta[h - k] A_\Delta^{-1}[k] = \mathbb{1}[h]. \quad (8)$$

where $\mathbb{1}[h] = 1$ when $h = 0$ and 0 otherwise. Taking the infinite DFT of both sides of (8) results in

$$A_\Delta(\omega) A_\Delta^{-1}(\omega) = \Delta^d, \quad (9)$$

meaning that the spectrum of A_Δ^{-1} is the Δ^d times the reciprocal of the spectrum of A_Δ .

We can also define the square root of A_Δ to be the operator $A_\Delta^{1/2}$ for which

$$A_\Delta[h] = \Delta^d \sum_{k \in \mathbb{Z}^d} A_\Delta^{1/2}[h - k] A_\Delta^{1/2}[-k] \quad (10)$$

Note the difference between (8), which is meant to mimic the matrix multiplication BB^{-1} , and (10), which is meant to mimic the matrix multiplication BB^T . Taking the Fourier transform of both sides reveals that

$$A_\Delta^{1/2}(\omega) A_\Delta^{1/2}(\omega)^* = A_\Delta(\omega), \quad (11)$$

where $*$ denotes complex conjugate. The spectral density of $A_\Delta^{1/2}$ is the complex square root of the spectral density of A_Δ . This means that the square root spectral density is unique only up to a multiple of $\exp(i\omega x)$. This is a necessary consequence of the translation-invariance property of stationary processes, since multiplication by $\exp(i\omega x)$ in the spectral domain corresponds to translation by x in the natural domain. Square root operators may also have inverses; their spectral densities again follow the reciprocal relationship.

Square root operators are useful for the simulation of processes that have particular covariances. Let $W : \mathbb{Z}^d \rightarrow \mathbb{R}$ be a white noise process defined on a the integer lattice (i.e. its autocovariance function is the identity function $\mathbb{1}[h]$). Define $Y : (\Delta\mathbb{Z})^d \rightarrow \mathbb{R}$ as

$$Y[\Delta j] = \Delta^{d/2} \sum_{k \in \mathbb{Z}^d} A_\Delta^{1/2}[j - k] W[k]. \quad (12)$$

The covariance function for Y is A_Δ . The representation in (12) is exploited in the convolution method of Higdon (1998).

The inverse of the square root operator can be used to decorrelate a process. For a process Y on $(\Delta\mathbb{Z})^d$ with autocovariance function A_Δ , let $A_\Delta^{-1/2}$ be the square root operator for A_Δ^{-1} , and define W on \mathbb{Z}^d as

$$W[j] = \Delta^{d/2} \sum_{k \in \mathbb{Z}^d} A_\Delta^{-1/2}[k-j] Y[\Delta k]. \quad (13)$$

The process W has covariance function $\mathbb{1}[h]$ and is thus a white noise process.

3 Matérn Covariances

The stationary Matérn covariance function is

$$M[h : \nu, d] = \frac{\sigma^2 (\alpha \|h\|)^\nu K_\nu(\alpha \|h\|)}{\Gamma(\nu) 2^{\nu-1}} = \int_{\mathbb{R}^d} \frac{\sigma^2 N_{\alpha, \nu, d}}{(\alpha^2 + 4\pi^2 \|\omega\|^2)^{\nu+d/2}} \exp(i2\pi\omega \cdot h) d\omega, \quad (14)$$

where $N_{\alpha, \nu, d}$ is a normalizing constant. Keeping with convention, we call σ^2 the variance parameter, α the inverse range parameter, and ν the smoothness parameter. The aliased spectral density is then

$$M_\Delta(\omega : \nu, d) = \sum_{k \in \mathbb{Z}^d} \frac{\sigma^2 N_{\alpha, \nu, d}}{(\alpha^2 + 4\pi^2 \|\omega + k/\Delta\|^2)^{\nu+d/2}}. \quad (15)$$

When $\nu + 1/2$ is an integer, the Matérn covariance is the product of a polynomial and an exponential. For example,

$$M[h : 1/2, d] = \sigma^2 \exp(-\alpha \|h\|), \quad (16)$$

$$M[h : 3/2, d] = \sigma^2 (1 + \alpha \|h\|) \exp(-\alpha \|h\|). \quad (17)$$

Our notation for M includes ν because we study approximations that involve Matérn functions with different values of ν .

3.1 One Dimension

From here on, we set $\sigma^2 = 1$ to simplify the expressions. When $d = 1$ and $\nu = 1/2$, the aliased spectral density has the closed form

$$M_\Delta(\omega : 1/2, 1) = \sum_{k \in \mathbb{Z}} \frac{N_{\alpha, 1/2, 1}}{\alpha^2 + 4\pi^2 (\omega + k/\Delta)^2} = \Delta \frac{1 - e^{-2\Delta\alpha}}{1 + e^{-2\Delta\alpha} - 2e^{-\Delta\alpha} \cos(\Delta 2\pi\omega)}. \quad (18)$$

This can be proven by taking the discrete Fourier transform of the covariance function. The inverse spectral density is simply the reciprocal

$$M_\Delta^{-1}(\omega : 1/2, 1) = \frac{1 + e^{-2\Delta\alpha} - 2e^{-\Delta\alpha} \cos(\Delta 2\pi\omega)}{1 - e^{-2\Delta\alpha}}, \quad (19)$$

and thus the inverse operator is

$$M_{\Delta}^{-1}[h : 1/2, 1] = \begin{cases} (1 + e^{-2\Delta\alpha})/(1 - e^{-2\Delta\alpha}) & h = 0, \\ -e^{-\Delta\alpha}/(1 - e^{-2\Delta\alpha}) & |h| = 1, \\ 0 & |h| > 1, \end{cases} \quad (20)$$

which can be shown by taking the Fourier transform of $M_{\Delta}^{-1}(\omega : 1/2, 1)$.

When $\nu = 3/2$, the aliased spectral density is

$$M_{\Delta}(\omega : 3/2, 1) = \sum_{k \in \mathbb{Z}} \frac{N_{\alpha, 3/2, 1}}{[\alpha^2 + 4\pi^2(\omega + k/\Delta)^2]^2} \quad (21)$$

which does have a simplified formula, but whose reciprocal does not. Further, the inverse operator is generally not sparse, which can be verified by numerical calculation. See Section 5 for details.

The SPDE sparse approximation in Lindgren et al. (2011) is

$$(1 - e^{-2\Delta\alpha})^2 \widetilde{M}_{\Delta}^{-1}[h : 1/2, 1] = \begin{cases} (1 + e^{-2\Delta\alpha})^2 + 2e^{-2\Delta\alpha} & h = 0 \\ -2(1 + e^{-2\Delta\alpha})e^{-\Delta\alpha} & |h| = 1 \\ e^{-2\Delta\alpha} & |h| = 2 \\ 0 & |h| > 2. \end{cases} \quad (22)$$

which corresponds to spectral density

$$\begin{aligned} \widetilde{M}_{\Delta}(\omega : 3/2, 1) &= M_{\Delta}(\omega : 1/2, 1)^2 = \left[\sum_{k \in \mathbb{Z}} \frac{N_{\alpha, 1/2, 1}}{\alpha^2 + 4\pi^2(\omega + k/\Delta)^2} \right]^2 \\ &= \sum_{k \in \mathbb{Z}} \sum_{j \in \mathbb{Z}} \frac{N_{\alpha, 1/2, 1}}{\alpha^2 + 4\pi^2(\omega + k/\Delta)^2} \frac{N_{\alpha, 1/2, 1}}{\alpha^2 + 4\pi^2(\omega + j/\Delta)^2} \end{aligned} \quad (23)$$

$$(24)$$

Therefore, comparing 21 to 24, the approximation error is

$$\frac{\widetilde{M}_{\Delta}(\omega : 3/2, 1)}{\widetilde{N}_{\alpha, 3/2, 1}} - \frac{M_{\Delta}(\omega : 3/2, 1)}{N_{\alpha, 3/2, 1}} = \sum_{k \in \mathbb{Z}} \sum_{j \neq k} \frac{1}{\alpha^2 + 4\pi^2(\omega + k/\Delta)^2} \frac{1}{\alpha^2 + 4\pi^2(\omega + j/\Delta)^2}, \quad (25)$$

where $\widetilde{N}_{\alpha, 3/2, 1} = N_{\alpha, 1/2, 1}^2$. In all of our results, we normalize the spectral densities by the factor that makes the approximation most accurate when $\alpha\Delta$ is small. It is of no consequence if an approximation differs by a constant factor, since all models have a variance term σ^2 that corrects for any scale changes introduced by an approximation. Theorem 1 establishes that the SPDE approximation becomes an increasingly accurate representation of the spectral density as $\alpha\Delta \rightarrow 0$.

Theorem 1. For all $\omega \in [0, 1/\Delta]$,

$$\left| \frac{\widetilde{M}_{\Delta}(\omega : 3/2, 1)}{\widetilde{N}_{\alpha, 3/2, 1}} - \frac{M_{\Delta}(\omega : 3/2, 1)}{N_{\alpha, 3/2, 1}} \right| \leq \frac{1}{\alpha^4} \left[\frac{\alpha^2 \Delta^2}{8} + \frac{\alpha^4 \Delta^4}{256} \right]. \quad (26)$$

The fact that the SPDE spectral density is a good approximation to the true spectral density does not imply that the approximation to the reciprocal of the spectral density is accurate. To provide insight into the reciprocal approximation, we study the behavior of the spectral density at the lowest frequency $\omega = 0$ and at the highest frequency $\omega = 1/(2\Delta)$, resulting in the following two theorems.

Theorem 2.

$$\left| \frac{M_{\Delta}(0 : 3/2, 1)}{N_{\alpha, 3/2, 1}} - \frac{1}{\alpha^4} \right| \leq \frac{1}{\alpha^4} \frac{\alpha^4 \Delta^4}{720} \quad (27)$$

$$\left| \frac{\widetilde{M}_{\Delta}(0 : 3/2, 1)}{\widetilde{N}_{\alpha, 3/2, 1}} - \frac{1}{\alpha^4} \right| \leq \frac{1}{\alpha^4} \left[\frac{\alpha^2 \Delta^2}{6} + \frac{\alpha^4 \Delta^4}{144} \right] \quad (28)$$

Theorem 3.

$$\frac{\widetilde{M}_{\Delta}(1/2\Delta : 3/2, 1)}{\widetilde{N}_{\alpha, 3/2, 1}} \geq 2 \frac{M_{\Delta}(1/2\Delta : 3/2, 1)}{N_{\alpha, 3/2, 1}} \quad (29)$$

Taken together, Theorems 2 and 3 imply that as $\alpha\Delta \rightarrow 0$, the two normalized spectral densities both converge to α^{-4} at $\omega = 0$, while the SPDE spectral density is at least twice as large as the true spectral density at $\omega = 1/(2\Delta)$. This means that the SPDE approximation differs from the true spectral density by a factor that varies substantially with frequency. In particular, the dynamic range of the SPDE approximation is too small by at least a factor of 2,

$$\frac{M_{\Delta}(0 : 3/2, 1)}{M_{\Delta}(1/2\Delta : 3/2, 1)} \gtrsim 2 \frac{\widetilde{M}_{\Delta}(0 : 3/2, 1)}{\widetilde{M}_{\Delta}(1/2\Delta : 3/2, 1)}, \quad (30)$$

where \gtrsim indicates that the inequality holds asymptotically as $\alpha\Delta \rightarrow 0$. The inaccuracy of the dynamic range impacts the quality of the approximation to the reciprocal of the spectral density and to the inverse operator. An example of how the SPDE can give an accurate approximation the spectral density but an inaccurate approximation to the reciprocal is plotted in Figure 1. The impact on the inverse operator is explored numerically in Section 5.

3.2 Two Dimensions

The aliased spectral density for the Matérn in two dimensions is

$$\frac{M_{\Delta}(\omega : \nu, 2)}{N_{a, \nu, 2}} = \sum_{k \in \mathbb{Z}^2} [\alpha^2 + 4\pi^2(\omega_1 + k_1/\Delta)^2 + 4\pi^2(\omega_2 + k_2/\Delta)^2]^{-\nu-1}. \quad (31)$$

The following theorem establishes that for $\nu = 1$, the spectral density at $\omega = (0, 0)$ is approximately α^{-4} , and it establishes upper bounds for the spectral density at the frequencies $\omega = (1/2\Delta, 0)$ and $\omega = (1/2\Delta, 1/2\Delta)$.

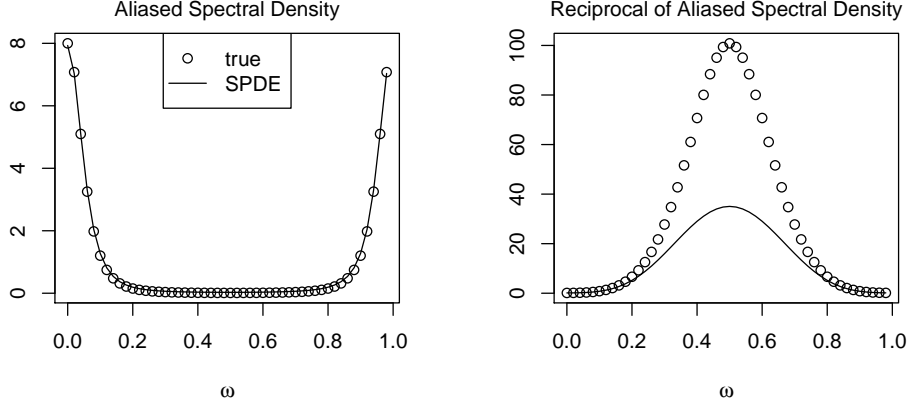


Figure 1: True aliased spectral density and its reciprocal (circles) and SPDE approximation to the aliased spectral density and its reciprocal.

Theorem 4.

$$\left| \frac{M_{\Delta}((0,0) : 1, 2)}{N_{a,1,2}} - \frac{1}{\alpha^4} \right| \leq \frac{1}{\alpha^4} \frac{\alpha^4 \Delta^4}{258.6} \quad (32)$$

$$\frac{M_{\Delta}((\frac{1}{2\Delta}, 0) : 1, 2)}{N_{a,1,2}} \leq \frac{1}{\alpha^4} \frac{\alpha^4 \Delta^4}{43.10} \quad (33)$$

$$\frac{M_{\Delta}((\frac{1}{2\Delta}, \frac{1}{2\Delta}) : 1, 2)}{N_{a,1,2}} \leq \frac{1}{\alpha^4} \frac{\alpha^4 \Delta^4}{86.20} \quad (34)$$

The numbers 258.6, 43.10, and 86.20 are the result of numerical calculations and are rounded to one or two decimals. They are available to higher accuracy. Details are given in the proof in Appendix B. The SPDE approximation is

$$\alpha^2 \Delta^2 \widetilde{M}_{\Delta}^{-1}[h : 1, 2] = \begin{cases} (4 + \alpha^2 \Delta^2)^2 + 4 & h = (0, 0) \\ -2(4 + \alpha^2 \Delta^2) & h = (0, 1), (0, -1), (1, 0), (-1, 0) \\ 2 & h = (1, 1), (1, -1), (-1, 1), (-1, -1) \\ 1 & h = (2, 0), (0, 2), (-2, 0), (0, -2) \\ 0 & \text{otherwise,} \end{cases} \quad (35)$$

which corresponds to the spectral density approximation,

$$\frac{\widetilde{M}_{\Delta}(\omega : 1, 2)}{\widetilde{N}_{\alpha,1,2}} = \Delta^4 \left(4 + \alpha^2 \Delta^2 - e^{i2\pi\Delta\omega_1} - e^{-i2\pi\Delta\omega_1} - e^{i2\pi\Delta\omega_2} - e^{-i2\pi\Delta\omega_2} \right)^{-2}. \quad (36)$$

The following theorem establishes the behavior of \widetilde{M}_{Δ} at $\omega = (0, 0)$, $\omega = (1/2\Delta, 0)$, and $\omega = (1/2\Delta, 1/2\Delta)$.

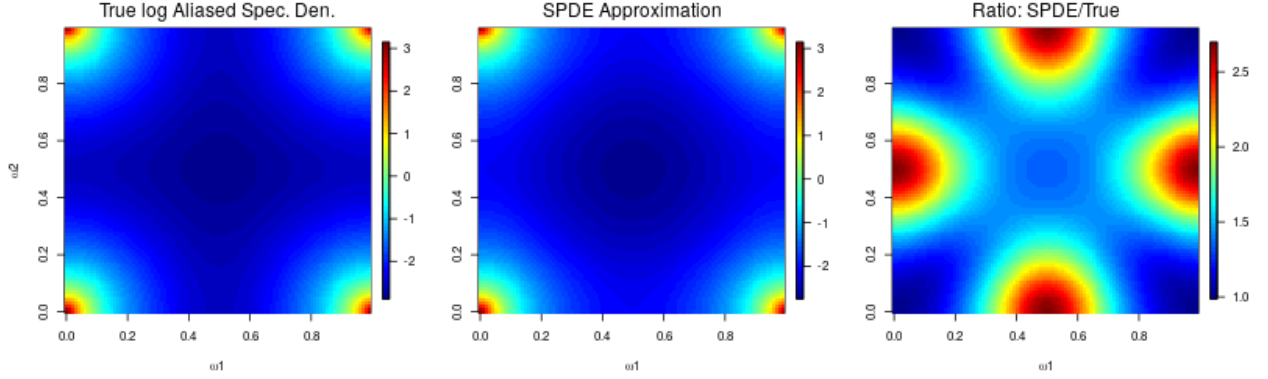


Figure 2: True spectral density for $\nu = 1$, $a = 0.5$, SPDE approximation to the spectral density, and the ratio of the two. The ratio is near 1.00 at $(0, 0)$, near 2.69 at $(1/2\Delta, 0)$ and near 1.35 at $(1/2\Delta, 1/2\Delta)$, as predicted by the theory.

Theorem 5.

$$\frac{\widetilde{M}_\Delta((0, 0) : 1, 2)}{\widetilde{N}_{\alpha, 1, 2}} = \frac{1}{\alpha^4} \quad (37)$$

$$\frac{\widetilde{M}_\Delta((\frac{1}{2\Delta}, 0) : 1, 2)}{\widetilde{N}_{\alpha, 1, 2}} = \frac{1}{\alpha^4} \frac{\alpha^4 \Delta^4}{(4 + \alpha^2 \Delta^2)^2} = \frac{1}{\alpha^4} \frac{\alpha^4 \Delta^4}{16} \left(1 - \frac{\alpha^2 \Delta^2}{2} + O(\alpha^4 \Delta^4)\right) \quad (38)$$

$$\frac{\widetilde{M}_\Delta((\frac{1}{2\Delta}, \frac{1}{2\Delta}) : 1, 2)}{\widetilde{N}_{\alpha, 1, 2}} = \frac{1}{\alpha^4} \frac{\alpha^4 \Delta^4}{(8 + \alpha^2 \Delta^2)^2} = \frac{1}{\alpha^4} \frac{\alpha^4 \Delta^4}{64} \left(1 - \frac{\alpha^2 \Delta^2}{4} + O(\alpha^4 \Delta^4)\right) \quad (39)$$

Theorems 4 and 5 imply that when $\alpha\Delta$ is small, the SPDE over-approximates the spectral density by a factor of $43.1/16 = 2.69$ at $\omega = (1/2\Delta, 0)$ and $86.2/64 = 1.35$ at $\omega = (1/2\Delta, 1/2\Delta)$. Figure 2 contains an example where the ratio between the SPDE spectral density and the true spectral density varies between 0.999 at $\omega = (0, 0)$, 2.680 at $\omega = (1/2\Delta, 0)$ and 1.345 at $\omega = (1/2\Delta, 1/2\Delta)$.

4 Computing The Operators

All of the operators we have mentioned—covariance, square root covariance, inverse, and square root inverse—are continuous Fourier transforms of elementary functions of the aliased spectral density over the domain $[0, 1/\Delta]$. Therefore, we can efficiently compute the operators if we can evaluate the aliased spectral density on a fine grid and numerically integrate simple functions of the spectral density. Fortunately, the Matérn has properties that allow for fast evaluation of the aliased spectral density, with the help of the Poisson summation formula, and numerical integration by a simple Riemann sum approximation is fast (with the FFT) and also accurate with a surprisingly small number of integration points.

4.1 Computing Spectral Density on a Fine Grid

Let $b = (b_1, \dots, b_d)$ be a vector of positive integers representing a grid size. Then define

$$\mathbb{J}(b_i) = \{0, 1, \dots, b_i - 1\} \quad \text{and} \quad \mathbb{J}(b) = \mathbb{J}(b_1) \times \dots \times \mathbb{J}(b_d), \quad (40)$$

so that $\mathbb{J}(b)$ is a set of points on a rectangular lattice. Let $\Delta\mathbb{J}(b)$ multiply each point in $\mathbb{J}(b)$ by Δ . Define

$$\mathbb{F}(b_i) = \left\{0, \frac{1}{b_i}, \dots, \frac{b_i - 1}{b_i}\right\} \quad \text{and} \quad \mathbb{F}(b) = \mathbb{F}(b_1) \times \dots \times \mathbb{F}(b_d). \quad (41)$$

This makes $\mathbb{F}(b)/\Delta$ the set of Fourier frequencies on $[0, 1/\Delta]^d$ for a grid of size b .

The Poisson summation formula (cf. Guinness and Fuentes, 2017) is

$$\sum_{k \in \mathbb{Z}^d} A(\omega + k/\Delta) = \sum_{h \in \Delta\mathbb{J}(b)} \left(\sum_{j \in \mathbb{Z}^d} A[h + \Delta b \circ j] \right) e^{i2\pi\omega \cdot h}, \quad \text{for all } \omega \in \mathbb{F}(b)/\Delta, \quad (42)$$

where \circ is elementwise multiplication. This means that we can compute the aliased spectral density by aliasing, or wrapping, the covariances, and then taking a finite discrete Fourier transform of the aliased covariances. We approximate the aliased covariances by truncating the sum over j in (42). For the Matérn model, aliasing the covariances is more computationally efficient than aliasing the spectral density, because the covariances have exponential decay, whereas the spectral densities have polynomial decay. This means that the truncated aliased covariances often converge after just a few terms in the sum.

4.2 Fourier Transforms

The inverse operator is

$$A_{\Delta}^{-1}[h] = \int_{[0, 1/\Delta]^d} \frac{\Delta^d e^{i2\pi\Delta\omega \cdot h}}{A_{\Delta}(\omega)} d\omega. \quad (43)$$

We approximate it with the Riemann sum

$$A_{\Delta, b}^{-1}[h] = \frac{1}{\Delta^d} \sum_{\omega \in \mathbb{F}(b)/\Delta} \frac{\Delta^d e^{i2\pi\Delta\omega \cdot h}}{A_{\Delta}(\omega)}, \quad (44)$$

which can be evaluated for all $h \in \mathbb{J}(b)$ quickly using an FFT. The integrand is a periodic function on the domain of integration. For Matérn models, the reciprocal of the aliased spectral density is infinitely differentiable and tends to be well-behaved even when Δ is very small. The periodicity and smoothness of the reciprocal spectral density makes the Riemann sum extremely accurate for small $\|h\|$. For Matérn covariances, the inverse operator for small $\|h\|$ is usually all that is required because the inverse operators tend to decay to zero very quickly as $\|h\|$ increases. Numerical results are given in Section 5.

4.3 KL-Divergence

The KL-divergence between two mean-zero multivariate normal distributions with covariance matrices Σ_0 and Σ_1 , with Σ_0 taken to be the truth, is

$$KL(\Sigma_0\|\Sigma_1) = \frac{1}{2} \left[\text{Tr}(\Sigma_1^{-1}\Sigma_0) + \log \det(\Sigma_1) - \log \det(\Sigma_0) - n \right]. \quad (45)$$

While the inverse operators for the Matérn are not exactly sparse—except when $d = 1$ and $\nu = 0.5$ —one can consider the most accurate approximation for a given sparsity level, where accuracy is judged by KL-divergence to the true model. This is explored in Section 5.

5 Numerical Results

This section contains results of numerical calculations and simulations meant to provide further insight into the inverse operators, SPDE approximations, and the KL-divergence-minimizing sparse approximations.

5.1 Dependence of Inverse Operator on Smoothness

In Figures 3 and 4, we plot

$$M_1^{-1}[h : \nu, d] / M_1^{-1}[0 : \nu, d] \quad (46)$$

for $d = 1, 2$, $\Delta = 1$, and for a range of values of smoothness parameter ν and inverse range α . First consider $d = 1$. When $h = 1$, the operator is always negative. When $h = 2$, the operator is exactly 0 for $\nu = 0.5$, agreeing with the theory from Section 3, which says that the operator is exactly zero when $\nu = 0.5$ for all $|h| > 1$. When $h = 3$, there is an additional zero near $\nu = 0.7$ but there is no zero at $\nu = 1.5$; the SPDE approximation sets the operator equal to zero when $\nu = 1.5$ for all $|h| > 2$. When $h = 4$, the only zero is at $\nu = 0.5$. For $d = 2$, the SPDE approximation sets the inverse operator to zero when $\nu = 1.0$ and $|h_1| + |h_2| > 2$. Figure 4 shows that while there are some zeros in the inverse operator, they generally do not appear at or near $\nu = 1.0$. For example, when $h = (1, 2)$, the inverse operator is nearly at its maximum when $\nu = 1.0$. While the magnitudes of the operators generally decrease as $\|h\|$ increases, there does not appear to be anything particularly sparse about the cases $d = 1, \nu = 3/2$ or $d = 2, \nu = 1$.

5.2 Numerical Evaluation of Approximations

We evaluate the entries and the KL-divergence of the SPDE approximation and our spectral and sparse approximations. KL-divergences are evaluated for models with periodic boundary conditions on a grid of size $b = (100)$ when dimension $d = 1$ and a grid of size $b = (100, 100)$ when dimension $d = 2$.

Figure 5 contains entries of the various approximations to the inverse operator for $d = 1$, $\Delta = 1$, $\nu = 3/2$, $a \in \{0.1, 0.4\}$. For the spectral approximation, we use $b = 100$ and truncate the aliasing of covariances after 16 terms. We define “SPDE A” to be the approximation

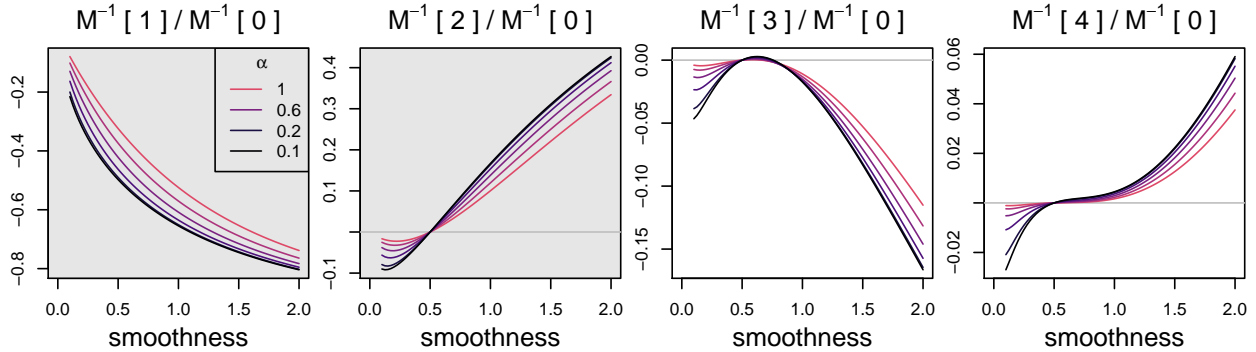


Figure 3: For dimension $d = 1$, entries of $M_1^{-1}[h]$ as a function of ν for various values of h and several inverse range parameters α . SPDE approximation sets inverse to zero when smoothness $\nu = 1.5$ in cases with white background.

that uses the specified value of inverse range α but chooses the variance σ^2 to minimize the KL-divergence to the true model. We define “SPDE B” to be the approximation that chooses both inverse range α and variance σ^2 to minimize KL-divergence. Therefore, SPDE B is necessarily more accurate (in terms of KL-divergence) than SPDE A. “Sparse 2” is an approximation with inverse operator equal to zero when $|h| > 2$, and thus has the same sparsity pattern as the SPDE approximation. “Sparse 3” is an approximation with inverse operator equal to zero when $|h| > 3$. Both are chosen to be the sparse approximation that minimizes KL-divergence. Therefore, Sparse 3 is necessarily more accurate than Sparse 2, and Sparse 2 is necessarily more accurate than SPDE B. Table 1 contains KL-divergences for the various approximations for a larger range of values of α . In all cases, we see that the spectral approximations are extremely accurate, and the approximations that are zero when $|h| > 2$ (SPDE A, SPDE B, and Sparse 2) are much less accurate than the approximations allow non-zero entries when $|h| = 3$.

Figure 6 contains analogous results for the $d = 2$ dimensional case. SPDE A and SPDE B have the same definition as in the one-dimensional case. “Sparse 2” is the best approximation that has inverse operator equal to zero when $|h_1| + |h_2| > 2$, and thus has the same sparsity pattern as the SPDE approximation. “Sparse 3” is the best approximation that has inverse operator equal to zero when $|h_1| + |h_2| > 3$. We observe the same features as in the one-dimensional case, with the Sparse 3 approximations providing a significant improvement to accuracy. One interesting observation is that the SPDE approximation always sets the $(1, 1)$ entry to be twice the $(0, 2)$ entry of the operator, whereas in the exact calculations, the $(1, 1)$ entry is roughly six times smaller than the $(0, 2)$ entry.

5.3 Simulation Study

We simulated two-dimensional data on a $(30, 30)$ grid under a Matérn model with $\sigma^2 = 2$, $\alpha = 0.2$, and $\nu = 1$. We assumed that the mean was known to be zero. We considered five estimation assumptions, all with known ν but unknown σ^2 and α :

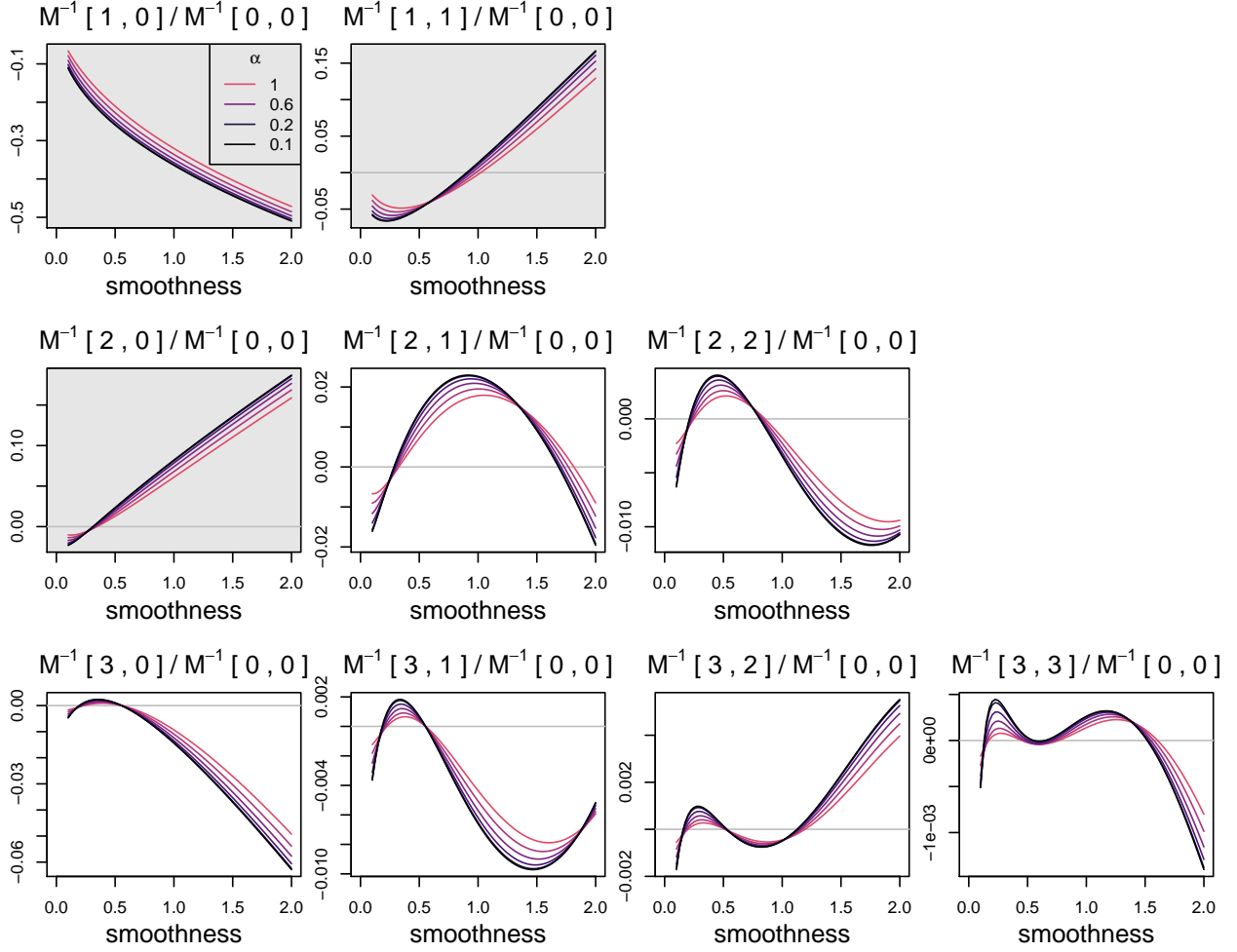


Figure 4: For dimension $d = 2$, entries of $M_1^{-1}[h]$ as a function of ν for various values of h and several inverse range parameters α . SPDE approximation sets inverse to zero when smoothness $\nu = 1.0$ in cases with white background.

a	1	0.8	0.6	0.4	0.2	0.1
Spectral	0.0000	0.0000	0.0000	0.0000	0.0000	0.0000
SPDE A	2.7786	3.0077	3.2000	3.3454	3.4360	3.4591
SPDE B	0.7380	1.0431	1.4476	1.9724	2.6387	3.0319
Sparse 2	0.2617	0.4548	0.7746	1.2956	2.1328	2.7280
Sparse 3	0.0149	0.0281	0.0508	0.0884	0.1483	0.1903

Table 1: KL-divergence on a size 100 grid when $d = 1$ and $\nu = 3/2$.

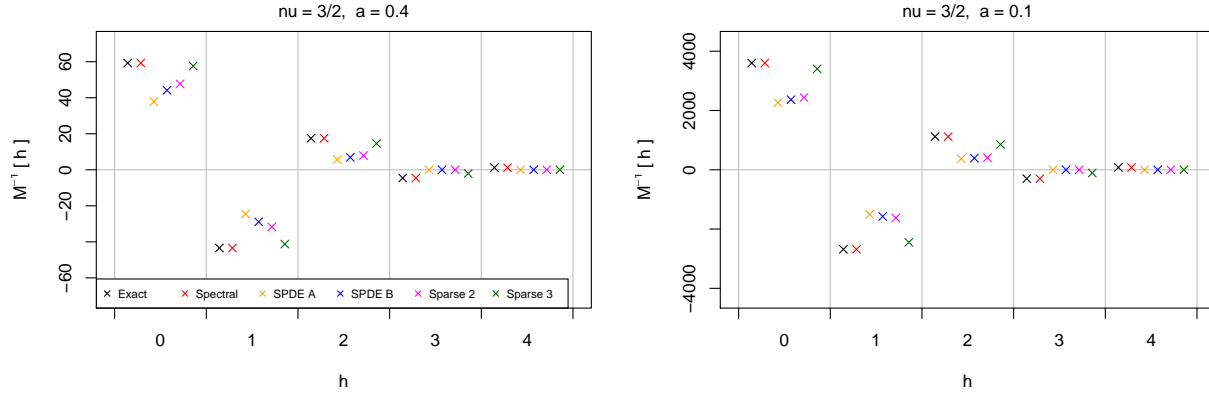


Figure 5: $M_1^{-1}[h]$ for $\alpha = 0.4$ and $\alpha = 0.1$. “Spectral” is the discrete spectral approximation, “SPDE A” is the best-fitting SPDE approximation for specified α , but allowing variance to vary, “SPDE B” is the best-fitting SPDE approximation over α and variance.

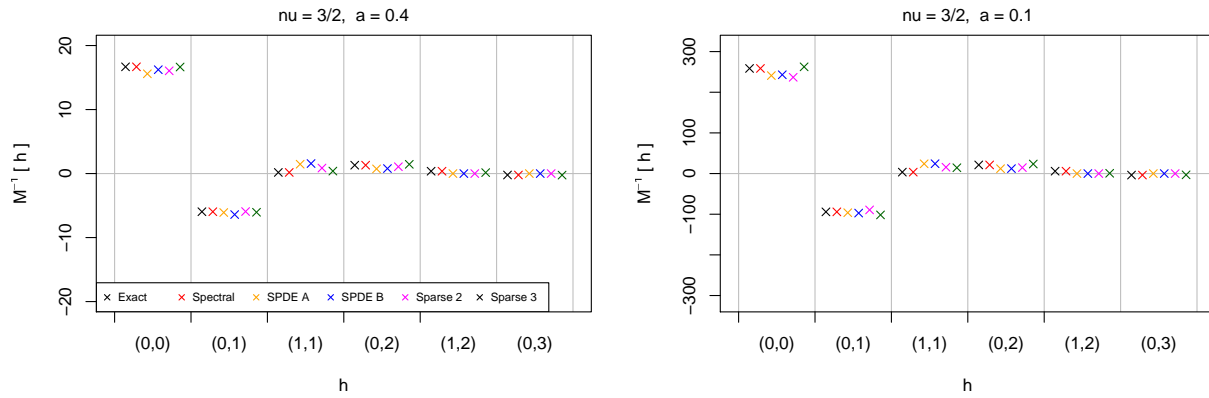


Figure 6: $M_1^{-1}[h]$ for $\alpha = 0.4$ and $\alpha = 0.1$. “Spectral” is the discrete spectral approximation, “SPDE A” is the best-fitting SPDE approximation for specified α , but allowing variance to vary, “SPDE B” is the best-fitting SPDE approximation over α and variance.

a	1	0.8	0.6	0.4	0.2	0.1
Spectral	0.0000	0.0000	0.0000	0.0000	0.0000	0.0000
SPDE A	76.4767	93.2476	108.3905	120.0517	127.0260	128.6811
SPDE B	54.5410	64.8624	77.1389	92.2475	111.0209	121.4407
Sparse 2	10.9230	16.5323	26.0552	42.6266	71.1521	91.3928
Sparse 3	0.9823	1.6123	2.4987	3.6559	9.6514	9.6905

Table 2: KL-divergence on a 100×100 grid with periodic boundary conditions when $d = 2$ and $\nu = 1$.

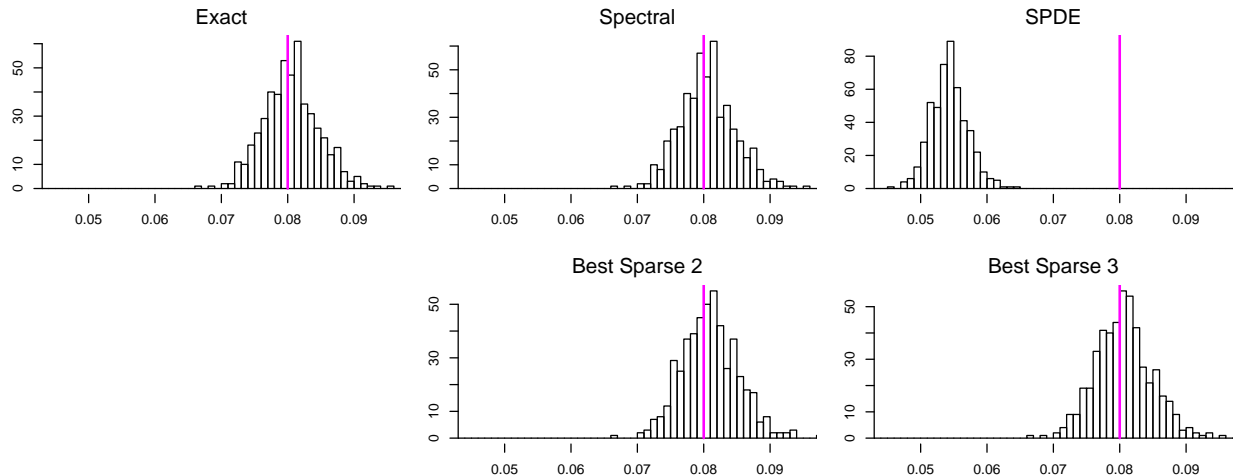


Figure 7: Histograms of $\hat{\sigma}^2\hat{\alpha}^2$, over 500 simulation replicates on a grid of size $(40, 40)$. True value $2(0.2)^2 = 0.08$ indicated in magenta.

1. true model,
2. Spectral approximation,
3. SPDE approximation,
4. Sparse 2 approximation,
5. Sparse 3 approximation.

For methods 2-5, we use the approximations to compute covariances under periodic boundary conditions on a $(50, 50)$ grid, and extract the covariances from the interior $(30, 30)$ grid. The SPDE approximation uses the coefficients in (35). The Sparse 2 approximation uses the same sparsity pattern as SPDE, but for a given (σ^2, α) , chooses the inverse operator coefficients that minimize the KL-divergence to the Matérn model. The Sparse 3 approximation does the same, except allows the inverse operator to be non-zero when $|h_1| + |h_2| = 3$. All parameters are estimated by maximum likelihood.

Figure 7 contains results of the simulation study over 500 simulation replicates. We plot histograms of microergodic parameter (Zhang, 2004) $\hat{\sigma}^2\hat{\alpha}^2$, and include a magenta line for the true value $2(0.2)^2 = 0.08$. We see that the exact, spectral, Sparse 2, and Sparse 3 methods provide accurate estimates of the microergodic parameter, but the SPDE approximation under-estimates it by more than 25% in most cases. This underestimation corresponds to an overestimation of the strength of the small-scale spatial dependence, since α is an inverse range parameter.

6 Discussion

The SPDE approximation has proven to be useful as a computational tool and as a conceptual tool for defining extensions to irregularly-spaced data, models on manifolds, and to non-stationary models (Fuglstad et al., 2015; Bakka et al., 2018). This paper does not question the usefulness of the SPDE approach as a tool for data analysis. Rather, it is a study of the ability of the SPDE approach to approximate Matérn models on grids. While this paper only studies properties of the covariance operators on grids, it would be interesting to explore whether the KL-divergence-minimizing sparse approximations can be ported to triangulated domains using the techniques developed by Lindgren et al. (2011).

Although not explored here, the KL-divergence-minimizing sparse approximations can be applied to Matérn models with any value of the smoothness parameter, and to any covariance function for that matter. It would be interesting to pursue further research on the accuracy of these sparse approximations, and on algorithms for quickly finding the KL-divergence-minimizing coefficients, since we found that the optimization was tricky; we had to give it good starting values and restart the algorithms when they failed to converge. The extension to arbitrary smoothness parameter would significantly expand the usefulness of sparse inverse approximations. Indeed, the limitation of the SPDE approximation to integer-valued smoothness parameters was noted in several of the discussions of the original paper. Based on the results shown in Figures 3 and 4, we expect that the sparse approximations will more or less uniformly worsen as ν increases.

The SPDE approximation has the benefit that it does not require evaluation of a Bessel function, whereas the spectral approximation and the sparse KL-divergence-minimizing approximations do. We note that the approximations explored here require evaluation of arrays of covariances only on the computation grid; if the grid has n points, they require a small multiple of n Bessel evaluations. This is opposed to filling in an entire $n \times n$ covariance matrix for irregularly spaced data, which would require n^2 Bessel evaluations. We expect that the factoring of large sparse inverse covariance matrices will dominate the computation time. Nevertheless, there may be some scope for simpler approximations that improve on the SPDE approximation without requiring Bessel evaluations. Figure 1, indicates that multiplying the reciprocal of the SPDE spectrum by a linear combination of 1 and $\cos(2\pi\Delta\omega)$ may significantly improve the approximation to the reciprocal. This would add an additional non-zero in the inverse operator. Similarly, in the $d = 2$ case, multiplying the reciprocal of the SPDE spectrum by a linear combination of 1, $\cos(2\pi\Delta\omega_1)$, $\cos(2\pi\Delta\omega_2)$, and $\cos(2\pi\Delta(\omega_1 + \omega_2))$, may significantly improve the approximation at the expense of adding non-zeros to the inverse operator.

Supplementary Material

The appendices contain additional background and proofs. R code for reproducing all numerical results and figures has been uploaded as online supplementary material.

Acknowledgements

This work was supported by the National Science Foundation under grant No. 1916208 and the National Institutes of Health under grant No. R01ES027892. The author is grateful to have received helpful feedback on an early draft from Matthias Katzfuss, Michael Stein, and Ethan Anderes.

A Extended Background

The first proposition establishes the aliasing property of complex exponential and uses it to express the covariances as an integral on a bounded domain instead of an infinite domain.

Proposition 1. (*Aliasing*) For $h \in \mathbb{Z}^d$,

$$A[\Delta h] = \int_{\mathbb{T}_\Delta^d} \left[\sum_{k \in \mathbb{Z}^d} A(\omega + k/\Delta) \right] \exp(i2\pi\Delta\omega \cdot h) d\omega \quad (47)$$

Proof. Using Bochner's theorem and splitting the integral into domains of size \mathbb{T}_Δ^d ,

$$A[\Delta h] = \sum_{k \in \mathbb{Z}^d} \int_{\mathbb{T}_\Delta^d} A(\omega + k/\Delta) \exp(i2\pi(\omega + k/\Delta) \cdot \Delta h) d\omega. \quad (48)$$

Exchanging sum with integral gives

$$A[\Delta h] = \int_{\mathbb{T}_\Delta^d} \sum_{k \in \mathbb{Z}^d} A(\omega + k/\Delta) \exp(i2\pi(\omega + k/\Delta) \cdot \Delta h) d\omega. \quad (49)$$

The complex exponential can be expanded as

$$\exp(i2\pi(\omega + k/\Delta) \cdot \Delta h) = \exp(i2\pi\Delta\omega \cdot h + i2\pi k \cdot h) = \exp(i2\pi\Delta\omega \cdot h) \exp(i2\pi k \cdot h). \quad (50)$$

Since $k \in \mathbb{Z}^2$ and $h \in \mathbb{Z}^2$, $k \cdot h = n$ is an integer, and thus the complex exponential is

$$\exp(i2\pi\Delta\omega \cdot h) \exp(i2\pi n) = \exp(i2\pi\Delta\omega \cdot h). \quad (51)$$

Plugging this expression back into the integral gives

$$A[\Delta h] = \int_{\mathbb{T}_\Delta^d} \left[\sum_{k \in \mathbb{Z}^d} A(\omega + k/\Delta) \right] \exp(i2\pi\Delta\omega \cdot h) d\omega, \quad (52)$$

as desired. □

The second proposition establishes the reciprocal relationship between the spectral density of the covariance operator and the spectral density of the inverse operator.

Proposition 2. (*Reciprocal Relationship of Inverse*) For all $\omega \in \mathbb{T}_\Delta^d$,

$$A_\Delta(\omega)A_\Delta^{-1}(\omega) = \Delta^d. \quad (53)$$

Proof. By definition, the inverse satisfies

$$\Delta^d \sum_{k \in \mathbb{Z}^d} A_\Delta[h-k] A_\Delta^{-1}[k] = \mathbb{1}[h]. \quad (54)$$

Take the infinite DFT of both sides,

$$\Delta^{2d} \sum_{h \in \mathbb{Z}^d} \sum_{k \in \mathbb{Z}^d} A_\Delta[h-k] A_\Delta^{-1}[k] e^{-i2\pi\Delta\omega \cdot h} = \Delta^d \sum_{h \in \mathbb{Z}^d} \mathbb{1}[h] e^{-i2\pi\Delta\omega \cdot h} \quad (55)$$

$$\Delta^d \sum_{k \in \mathbb{Z}^d} A_\Delta^{-1}[k] e^{-i2\pi\Delta\omega \cdot k} \Delta^d \sum_{h \in \mathbb{Z}^d} A_\Delta[h-k] e^{-i2\pi\Delta\omega \cdot (h-k)} = \Delta^d \quad (56)$$

$$A_\Delta^{-1}(\omega) A_\Delta(\omega) = \Delta^d. \quad (57)$$

□

Proposition 3. (*Square Root spectral density*) For all $\omega \in \mathbb{T}_\Delta^d$,

$$A_\Delta^{1/2}(\omega) A_\Delta^{1/2}(\omega)^* = A_\Delta(\omega). \quad (58)$$

Proof. By definition, the square root operator satisfies

$$\Delta^d \sum_{k \in \mathbb{Z}^d} A_\Delta^{1/2}[h-k] A_\Delta^{1/2}[-k] = A_\Delta[h]. \quad (59)$$

Taking the infinite DFT of both sides,

$$\Delta^{2d} \sum_{h \in \mathbb{Z}^d} \sum_{k \in \mathbb{Z}^d} A_\Delta^{1/2}[h-k] A_\Delta^{1/2}[-k] e^{-i2\pi\Delta\omega \cdot h} = \Delta^d \sum_{h \in \mathbb{Z}^d} A_\Delta[h] e^{-i2\pi\Delta\omega \cdot h} \quad (60)$$

$$\Delta^d \sum_{k \in \mathbb{Z}^d} A_\Delta^{1/2}[-k] e^{-i2\pi\Delta\omega \cdot k} \Delta^d \sum_{h \in \mathbb{Z}^d} A_\Delta^{1/2}[h-k] e^{-i2\pi\Delta\omega \cdot (h-k)} = A_\Delta(\omega) \quad (61)$$

$$A_\Delta^{1/2}(\omega) A_\Delta^{1/2}(\omega)^* = A_\Delta(\omega). \quad (62)$$

□

Proposition 4. (*Convolution Method of Simulation*) If the mean-zero process $W : \mathbb{Z}^d \rightarrow \mathbb{R}$ has covariance operator $\mathbb{1}[h]$, and

$$Y[\Delta h] = \Delta^{d/2} \sum_{k \in \mathbb{Z}^d} A_\Delta^{1/2}[h-k] W[k], \quad (63)$$

then $\text{Cov}(Y[\Delta h], Y[\Delta j]) = A_\Delta[h-j]$.

Proof.

$$\text{Cov}(Y[\Delta h], Y[\Delta j]) = E \left[\Delta^{d/2} \sum_{k \in \mathbb{Z}^d} A_\Delta^{1/2}[h-k] W[k] \Delta^{d/2} \sum_{m \in \mathbb{Z}^d} A_\Delta^{1/2}[j-m] W[m] \right] \quad (64)$$

$$= \Delta^d \sum_{k \in \mathbb{Z}^d} A_\Delta^{1/2}[h-k] A_\Delta^{1/2}[j-k] \quad (65)$$

$$= \Delta^d \sum_{\ell \in \mathbb{Z}^d} A_\Delta^{1/2}[h-j-\ell] A_\Delta^{1/2}[-\ell] \quad (66)$$

$$= A_\Delta[h-j]. \quad (67)$$

□

Proposition 5. *If the mean-zero process $Y : (\Delta\mathbb{Z})^d \rightarrow \mathbb{R}$ has covariance operator A_Δ , and*

$$W[h] = \Delta^{d/2} \sum_{k \in \mathbb{Z}^d} A_\Delta^{-1/2}[h - k] Y[\Delta k], \quad (68)$$

then $\text{Cov}(W[h], W[j]) = \mathbb{1}[h - j]$.

Proof.

$$\text{Cov}(W[h], W[j]) \quad (69)$$

$$= E \left[\Delta^{d/2} \sum_{k \in \mathbb{Z}^d} A_\Delta^{-1/2}[h - k] Y[\Delta k] \Delta^{d/2} \sum_{m \in \mathbb{Z}^d} A_\Delta^{-1/2}[j - m] Y[\Delta m] \right] \quad (70)$$

$$= \Delta^d \sum_{k \in \mathbb{Z}^d} \sum_{m \in \mathbb{Z}^d} A_\Delta^{-1/2}[h - k] A_\Delta^{-1/2}[j - m] A_\Delta[m - k] \quad (71)$$

$$= \Delta^d \sum_{k \in \mathbb{Z}^d} \sum_{m \in \mathbb{Z}^d} A_\Delta^{-1/2}[h - k] A_\Delta^{-1/2}[j - m] \Delta^d \sum_{\ell \in \mathbb{Z}^d} A_\Delta^{1/2}[m - k - \ell] A_\Delta^{1/2}[-\ell] \quad (72)$$

$$= \Delta^d \sum_{k \in \mathbb{Z}^d} \sum_{\ell \in \mathbb{Z}^d} A_\Delta^{-1/2}[h - k] A_\Delta^{1/2}[-\ell] \Delta^d \sum_{m \in \mathbb{Z}^d} A_\Delta^{1/2}[m - k - \ell] A_\Delta^{-1/2}[j - m] \quad (73)$$

$$= \Delta^d \sum_{k \in \mathbb{Z}^d} \sum_{\ell \in \mathbb{Z}^d} A_\Delta^{-1/2}[h - k] A_\Delta^{1/2}[-\ell] \Delta^d \sum_{n \in \mathbb{Z}^d} A_\Delta^{1/2}[j - k - \ell - n] A_\Delta^{-1/2}[n] \quad (74)$$

$$= \Delta^d \sum_{k \in \mathbb{Z}^d} \sum_{\ell \in \mathbb{Z}^d} A_\Delta^{-1/2}[h - k] A_\Delta^{1/2}[-\ell] \mathbb{1}[j - k - \ell] \quad (75)$$

$$= \Delta^d \sum_{k \in \mathbb{Z}^d} A_\Delta^{-1/2}[h - k] A_\Delta^{1/2}[k - j] \quad (76)$$

$$= \mathbb{1}[h - j] \quad (77)$$

□

B Proofs for Matérn Model

The proofs are simpler if we evaluate the aliased spectral densities on $[-1/2\Delta, 1/2\Delta]$ instead of $[0, 1/\Delta]$. This is of no consequence because the aliased spectral densities are periodic with period $1/\Delta$.

B.1 One Dimension

Lemma 1. *For all $\omega \in [-1/2\Delta, 1/2\Delta]$,*

$$\sum_{k=1}^{\infty} \left(1 + \frac{4\pi^2}{\alpha^2} (\omega \pm k/\Delta)^2 \right)^{-1} \leq \frac{\alpha^2 \Delta^2}{32}. \quad (78)$$

Proof. For all $\omega \in [-1/2\Delta, 1/2\Delta]$ and $k > 0$,

$$|\omega + k/\Delta| \geq \frac{1}{\Delta} |2k - 1| \quad \text{and} \quad |\omega - k/\Delta| \geq \frac{1}{\Delta} |1 - 2k|. \quad (79)$$

Therefore,

$$\sum_{k=1}^{\infty} \left(1 + \frac{4\pi^2}{\alpha^2} (\omega \pm k/\Delta)^2\right)^{-1} \leq \sum_{k=1}^{\infty} \frac{\alpha^2}{4\pi^2} |\omega \pm k/\Delta|^{-2} \quad (80)$$

$$\leq \frac{\alpha^2 \Delta^2}{4\pi^2} \sum_{k=1}^{\infty} |2k-1|^{-2} \quad (81)$$

$$= \frac{\alpha^2 \Delta^2}{4\pi^2} \frac{\pi^2}{8} = \frac{\alpha^2 \Delta^2}{32}. \quad (82)$$

□

Theorem 1. For all $\omega \in [-1/2\Delta, 1/2\Delta]$,

$$\left| \frac{\widetilde{M}_{\Delta}(\omega : 3/2, 1)}{\widetilde{N}_{\alpha, 3/2, 1}} - \frac{M_{\Delta}(\omega : 3/2, 1)}{N_{\alpha, 3/2, 1}} \right| \leq \frac{1}{\alpha^4} \left[\frac{\alpha^2 \Delta^2}{8} + \frac{\alpha^4 \Delta^4}{256} \right]. \quad (83)$$

Proof. Recall that the approximation error is

$$\frac{\widetilde{M}_{\Delta}(\omega : 3/2, 1)}{\widetilde{N}_{\alpha, 3/2, 1}} - \frac{M_{\Delta}(\omega : 3/2, 1)}{N_{\alpha, 3/2, 1}} = \sum_{\{k, j \in \mathbb{Z} : k \neq j\}} [\alpha^2 + 4\pi^2(\omega + k/\Delta)^2]^{-1} [\alpha^2 + 4\pi^2(\omega + j/\Delta)^2]^{-1} \quad (84)$$

Split the summation set into disjoint sets as

$$\{k, j \in \mathbb{Z} : k \neq j\} = \{j = 0, k \neq 0\} \cup \{k = 0, j \neq 0\} \cup \quad (85)$$

$$\{k > 0, j > 0, k \neq j\} \cup \{k < 0, j > 0, k \neq j\} \quad (86)$$

$$\{k > 0, j < 0, k \neq j\} \cup \{k < 0, j < 0, k \neq j\}, \quad (87)$$

then evaluate each summation individually.

$$S_1 = \sum_{\{j=0, k \neq 0\}} \left(\alpha^2 + 4\pi^2(\omega + k/\Delta)^2\right)^{-1} \left(\alpha^2 + 4\pi^2(\omega + j/\Delta)^2\right)^{-1} \quad (88)$$

$$= \frac{1}{\alpha^4} \left(1 + \frac{4\pi^2 \omega^2}{\alpha^2}\right)^{-1} \left[\sum_{k=1}^{\infty} \left(1 + \frac{4\pi^2}{\alpha^2} (\omega + k/\Delta)^2\right)^{-1} + \sum_{k=1}^{\infty} \left(1 + \frac{4\pi^2}{\alpha^2} (\omega - k/\Delta)^2\right)^{-1} \right] \quad (89)$$

$$\leq \frac{1}{\alpha^4} \frac{\alpha^2 \Delta^2}{16}, \quad (90)$$

which uses Lemma 1. The exact same derivation shows that

$$S_2 = \sum_{\{k=0, j \neq 0\}} \left(\alpha^2 + (\omega + 2\pi k/\Delta)^2\right)^{-1} \left(\alpha^2 + (\omega + 2\pi j/\Delta)^2\right)^{-1} \leq \frac{1}{\alpha^4} \frac{\alpha^2 \Delta^2}{16}. \quad (91)$$

The next term is

$$S_3 = \sum_{\{k>0, j>0, k \neq j\}} \left(\alpha^2 + (\omega + 2\pi k/\Delta)^2 \right)^{-1} \left(\alpha^2 + (\omega + 2\pi j/\Delta)^2 \right)^{-1} \quad (92)$$

$$\leq \frac{1}{\alpha^4} \sum_{k=1}^{\infty} \sum_{j=1}^{\infty} \left(1 + \frac{4\pi^2}{\alpha^2} (\omega + k/\Delta)^2 \right)^{-1} \left(1 + \frac{4\pi^2}{\alpha^2} (\omega + j/\Delta)^2 \right)^{-1} \quad (93)$$

$$\leq \frac{1}{\alpha^4} \sum_{k=1}^{\infty} \left(1 + \frac{4\pi^2}{\alpha^2} (\omega + k/\Delta)^2 \right)^{-1} \sum_{j=1}^{\infty} \left(1 + \frac{4\pi^2}{\alpha^2} (\omega + j/\Delta)^2 \right)^{-1} \quad (94)$$

$$\leq \frac{1}{\alpha^4} \frac{\alpha^2 \Delta^2}{32} \frac{\alpha^2 \Delta^2}{32} = \frac{1}{\alpha^4} \frac{\alpha^4 \Delta^4}{1024}, \quad (95)$$

which again uses Lemma 1. Nearly the exact same derivations show that the remaining sums have the same bound. Adding these bounds together gives

$$\sum_{\{k, j \in \mathbb{Z} : k \neq j\}} \left(\alpha^2 + (\omega + 2\pi k/\Delta)^2 \right)^{-1} \left(\alpha^2 + (\omega + 2\pi j/\Delta)^2 \right)^{-1} \leq \frac{2}{\alpha^4} \frac{\alpha^2 \Delta^2}{16} + \frac{4}{\alpha^4} \frac{\alpha^4 \Delta^4}{1024} \quad (96)$$

$$= \frac{1}{\alpha^4} \left[\frac{\alpha^2 \Delta^2}{8} + \frac{\alpha^4 \Delta^4}{256} \right]. \quad (97)$$

□

Lemma 2. For all $\omega \in [-1/2\Delta, 1/2\Delta]$,

$$\sum_{k=1}^{\infty} \left(1 + \frac{4\pi^2}{\alpha^2} (k/\Delta)^2 \right)^{-1} \leq \frac{\alpha^2 \Delta^2}{24}, \quad (98)$$

$$\sum_{k=1}^{\infty} \left(1 + \frac{4\pi^2}{\alpha^2} (k/\Delta)^2 \right)^{-2} \leq \frac{\alpha^4 \Delta^4}{1440}, \quad (99)$$

$$(100)$$

Proof. The first is

$$\sum_{k=1}^{\infty} \left[1 + \frac{4\pi^2}{\alpha^2 \Delta^2} k^2 \right]^{-1} \leq \frac{\alpha^2 \Delta^2}{4\pi^2} \sum_{k=1}^{\infty} k^{-2} = \frac{\alpha^2 \Delta^2}{4\pi^2} \frac{\pi^2}{6} = \frac{\alpha^2 \Delta^2}{24} \quad (101)$$

The second is

$$\sum_{k=1}^{\infty} \left[1 + \frac{4\pi^2}{\alpha^2 \Delta^2} k^2 \right]^{-2} \leq \frac{\alpha^4 \Delta^4}{16\pi^4} \sum_{k=1}^{\infty} k^{-4} = \frac{\alpha^4 \Delta^4}{16\pi^4} \frac{\pi^4}{90} = \frac{\alpha^4 \Delta^4}{1440} \quad (102)$$

□

Theorem 2.

$$\left| \frac{M_{\Delta}(0 : 3/2, 1)}{N_{\alpha, 3/2, 1}} - \frac{1}{\alpha^4} \right| \leq \frac{1}{\alpha^4} \frac{\alpha^4 \Delta^4}{720} \quad (103)$$

$$\left| \frac{\widetilde{M}_{\Delta}(0 : 3/2, 1)}{\widetilde{N}_{\alpha, 3/2, 1}} - \frac{1}{\alpha^4} \right| \leq \frac{1}{\alpha^4} \left[\frac{\alpha^2 \Delta^2}{6} + \frac{\alpha^4 \Delta^4}{144} \right] \quad (104)$$

Proof. To prove the first bound,

$$\left| \frac{M_{\Delta}(0 : 3/2, 1)}{N_{\alpha, 3/2, 1}} - \frac{1}{\alpha^4} \right| = \sum_{k \neq 0} (\alpha^2 + 4\pi^2(0 + k/\Delta)^2)^{-2} \quad (105)$$

$$= \frac{2}{\alpha^4} \sum_{k=1}^{\infty} \left(1 + \frac{4\pi^2}{\alpha^2} (k/\Delta)^2 \right)^{-2} \quad (106)$$

$$= \frac{1}{\alpha^4} \frac{\alpha^4 \Delta^4}{720}. \quad (107)$$

The second bound can be written as

$$\left| \frac{\widetilde{M}_{\Delta}(0 : 3/2, 1)}{\widetilde{N}_{\alpha, 3/2, 1}} - \frac{1}{\alpha^4} \right| = \sum_{\{k, j \in \mathbb{Z} : (j, k) \neq (0, 0)\}} \frac{1}{\alpha^4} \left[1 + \frac{4\pi^2}{\alpha^2} (j/\Delta)^2 \right]^{-1} \left[1 + \frac{4\pi^2}{\alpha^2} (k/\Delta)^2 \right]^{-1}. \quad (108)$$

Split the summation set into parts

$$\{k, j \in \mathbb{Z} : (j, k) \neq (0, 0)\} = \{j = 0, k \neq 0\} \cup \{k = 0, j \neq 0\} \cup \quad (109)$$

$$\{j > 0, k > 0\} \cup \{j < 0, k > 0\} \cup \quad (110)$$

$$\{j > 0, k < 0\} \cup \{j < 0, k < 0\}, \quad (111)$$

and evaluate each sum individually.

$$S_1 = \frac{1}{\alpha^4} \sum_{k \neq 0} \left(1 + \frac{4\pi^2}{\alpha^2} (k/\Delta)^2 \right)^{-1} \leq \frac{2}{\alpha^4} \frac{\alpha^2 \Delta^2}{24} = \frac{1}{\alpha^4} \frac{\alpha^2 \Delta^2}{12}, \quad (112)$$

which uses Lemma 2. The second term is bounded exactly the same way. The third term is

$$S_3 = \sum_{j=1}^{\infty} \sum_{k=1}^{\infty} (\alpha^2 + 4\pi^2(j/\Delta)^2)^{-1} (\alpha^2 + 4\pi^2(k/\Delta)^2)^{-1} \quad (113)$$

$$= \frac{1}{\alpha^4} \sum_{j=1}^{\infty} \left(1 + \frac{4\pi^2}{\alpha^2} (j/\Delta)^2 \right)^{-1} \sum_{k=1}^{\infty} \left(1 + \frac{4\pi^2}{\alpha^2} (k/\Delta)^2 \right)^{-1} \quad (114)$$

$$\leq \frac{1}{\alpha^4} \frac{\alpha^4 \Delta^4}{576}. \quad (115)$$

Adding these together yields the bound

$$\left| \frac{\widetilde{M}_{\Delta}(0 : 3/2, 1)}{\widetilde{N}_{\alpha, 3/2, 1}} - \frac{1}{\alpha^4} \right| \leq \frac{2}{\alpha^4} \frac{\alpha^2 \Delta^2}{12} + \frac{4}{\alpha^4} \frac{\alpha^4 \Delta^4}{576} = \frac{1}{\alpha^4} \left[\frac{\alpha^2 \Delta^2}{6} + \frac{\alpha^4 \Delta^4}{144} \right] \quad (116)$$

□

Theorem 3.

$$\frac{\widetilde{M}_{\Delta}(1/2\Delta : 3/2, 1)}{\widetilde{N}_{\alpha, 3/2, 1}} \geq 2 \frac{M_{\Delta}(1/2\Delta : 3/2, 1)}{N_{\alpha, 3/2, 1}} \quad (117)$$

Proof.

$$\frac{\widetilde{M}_\Delta(1/2\Delta : 3/2, 1)}{\widetilde{N}_{\alpha, 3/2, 1}} = \sum_{j \in \mathbb{Z}} \sum_{k \in \mathbb{Z}} \left[\alpha^2 + \frac{\pi^2}{\Delta^2} (2j+1)^2 \right]^{-1} \left[\alpha^2 + \frac{\pi^2}{\Delta^2} (2k+1)^2 \right]^{-1} \quad (118)$$

$$= \sum_{k \in \mathbb{Z}} \left[\alpha^2 + \frac{\pi^2}{\Delta^2} (2k+1)^2 \right]^{-2} + \sum_{k, j \in \mathbb{Z}: k \neq j} \left[\alpha^2 + \frac{\pi^2}{\Delta^2} (2j+1)^2 \right]^{-1} \left[\alpha^2 + \frac{\pi^2}{\Delta^2} (2k+1)^2 \right]^{-1} \quad (119)$$

$$\geq \frac{M_\Delta(1/2\Delta : 3/2, 1)}{N_{\alpha, 3/2, 1}} + \sum_{k=-\infty}^{\infty} \left[\alpha^2 + \frac{\pi^2}{\Delta^2} (2k+1)^2 \right]^{-1} \left[\alpha^2 + \frac{\pi^2}{\Delta^2} (2(-1-k)+1)^2 \right]^{-1} \quad (120)$$

$$= \frac{M_\Delta(1/2\Delta : 3/2, 1)}{N_{\alpha, 3/2, 1}} + \sum_{k=-\infty}^{\infty} \left[\alpha^2 + \frac{\pi^2}{\Delta^2} (2k+1)^2 \right]^{-1} \left[\alpha^2 + \frac{\pi^2}{\Delta^2} (-2k-1)^2 \right]^{-1} \quad (121)$$

$$= \frac{M_\Delta(1/2\Delta : 3/2, 1)}{N_{\alpha, 3/2, 1}} + \sum_{k=-\infty}^{\infty} \left[\alpha^2 + \frac{\pi^2}{\Delta^2} (2k+1)^2 \right]^{-2} \quad (122)$$

$$= 2 \frac{M_\Delta(1/2\Delta : 3/2, 1)}{N_{\alpha, 3/2, 1}}. \quad (123)$$

The inequality follows from the fact that $\{j, k : j + k = -1\} \subset \{j, k : j \neq k\}$. \square

B.2 Two Dimensions

Theorem 4.

$$\left| \frac{M_\Delta((0, 0) : 1, 2)}{N_{a, 1, 2}} - \frac{1}{\alpha^4} \right| \leq \frac{1}{\alpha^4} \frac{\alpha^4 \Delta^4}{258.6} \quad (124)$$

$$\frac{M_\Delta((\frac{1}{2\Delta}, 0) : 1, 2)}{N_{a, 1, 2}} \leq \frac{1}{\alpha^4} \frac{\alpha^4 \Delta^4}{43.10} \quad (125)$$

$$\frac{M_\Delta((\frac{1}{2\Delta}, \frac{1}{2\Delta}) : 1, 2)}{N_{a, 1, 2}} \leq \frac{1}{\alpha^4} \frac{\alpha^4 \Delta^4}{86.20} \quad (126)$$

Proof.

$$\left| \frac{M_\Delta((0, 0) : 1, 2)}{N_{a, 1, 2}} - \frac{1}{\alpha^4} \right| = \sum_{k \neq (0, 0)} \left[\alpha^2 + 4\pi^2 (k_1/\Delta)^2 + 4\pi^2 (k_2/\Delta)^2 \right]^{-2} \quad (127)$$

$$= \frac{1}{\alpha^4} \sum_{k \neq (0, 0)} \left[1 + \frac{4\pi^2 k_1^2}{\alpha^2 \Delta^2} + \frac{4\pi^2 k_2^2}{\alpha^2 \Delta^2} \right]^{-2} \quad (128)$$

$$\leq \frac{1}{\alpha^4} \frac{\alpha^4 \Delta^4}{16\pi^4} \sum_{k \neq (0, 0)} (k_1^2 + k_2^2)^{-2} \quad (129)$$

$$\approx \frac{1}{\alpha^4} \frac{\alpha^4 \Delta^4}{258.6}. \quad (130)$$

where \approx means that the sum was calculated numerically.

$$\frac{M_\Delta((\frac{1}{2\Delta}, 0) : 1, 2)}{N_{a,1,2}} = \sum_{k \in \mathbb{Z}^2} \left[\alpha^2 + 4\pi^2(1/2\Delta + k_1/\Delta)^2 + 4\pi^2(k_2/\Delta)^2 \right]^{-2} \quad (131)$$

$$= \frac{1}{\alpha^4} \sum_{k \in \mathbb{Z}^2} \left\{ 1 + \frac{4\pi^2}{\alpha^2 \Delta^2} \left[(k_1 + 1/2)^2 + k_2^2 \right] \right\}^{-2} \quad (132)$$

$$\leq \frac{1}{\alpha^4} \frac{\alpha^4 \Delta^4}{16\pi^4} \sum_{k \in \mathbb{Z}^2} \left[(k_1 + 1/2)^2 + k_2^2 \right]^{-2} \quad (133)$$

$$\approx \frac{1}{\alpha^4} \frac{\alpha^4 \Delta^4}{43.10}. \quad (134)$$

$$\frac{M_\Delta((\frac{1}{2\Delta}, \frac{1}{2\Delta}) : 1, 2)}{N_{a,1,2}} = \sum_{k \in \mathbb{Z}^2} \left[\alpha^2 + 4\pi^2(1/2\Delta + k_1/\Delta)^2 + 4\pi^2(1/2\Delta + k_2/\Delta)^2 \right]^{-2} \quad (135)$$

$$= \frac{1}{\alpha^4} \sum_{k \in \mathbb{Z}^2} \left\{ 1 + \frac{4\pi^2}{\alpha^2 \Delta^2} \left[(k_1 + 1/2)^2 + (k_2 + 1/2)^2 \right] \right\}^{-2} \quad (136)$$

$$\leq \frac{1}{\alpha^4} \frac{\alpha^4 \Delta^4}{16\pi^4} \sum_{k \in \mathbb{Z}^2} \left[(k_1 + 1/2)^2 + (k_2 + 1/2)^2 \right]^{-2} \quad (137)$$

$$\approx \frac{1}{\alpha^4} \frac{\alpha^4 \Delta^4}{86.20}. \quad (138)$$

□

Theorem 5.

$$\frac{\widetilde{M}_\Delta((0, 0) : 1, 2)}{\widetilde{N}_{a,1,2}} = \frac{1}{\alpha^4} \quad (139)$$

$$\frac{\widetilde{M}_\Delta((\frac{1}{2\Delta}, 0) : 1, 2)}{\widetilde{N}_{a,1,2}} = \frac{\Delta^4}{(4 + \alpha^2 \Delta^2)^2} = \frac{\Delta^4}{16} \left(1 - \frac{\alpha^2 \Delta^2}{2} + O(\alpha^4 \Delta^4) \right) \quad (140)$$

$$\frac{\widetilde{M}_\Delta((\frac{1}{2\Delta}, \frac{1}{2\Delta}) : 1, 2)}{\widetilde{N}_{a,1,2}} = \frac{\Delta^4}{(8 + \alpha^2 \Delta^2)^2} = \frac{\Delta^4}{64} \left(1 - \frac{\alpha^2 \Delta^2}{4} + O(\alpha^4 \Delta^4) \right) \quad (141)$$

Proof. The three equalities follow by plugging the frequency into the equation for the SPDE approximation to the spectral density. The only thing to prove are the big-O expressions.

$$\Delta^4(4 + \alpha^2 \Delta^2)^{-2} = \frac{\Delta^4}{16} \left(1 + \frac{\alpha^2 \Delta^2}{4} \right)^{-2} \quad (142)$$

$$= \frac{\Delta^4}{16} \left(1 - \frac{\alpha^2 \Delta^2}{4} + O(\alpha^4 \Delta^4) \right)^2 \quad (143)$$

$$= \frac{\Delta^4}{16} \left(1 - \frac{\alpha^2 \Delta^2}{2} + O(\alpha^4 \Delta^4) \right) \quad (144)$$

$$\Delta^4(8 + \alpha^2\Delta^2)^{-2} = \frac{\Delta^4}{64} \left(1 + \frac{\alpha^2\Delta^2}{8}\right)^{-2} \quad (145)$$

$$= \frac{\Delta^4}{64} \left(1 - \frac{\alpha^2\Delta^2}{8} + O(\alpha^4\Delta^4)\right)^2 \quad (146)$$

$$= \frac{\Delta^4}{64} \left(1 - \frac{\alpha^2\Delta^2}{4} + O(\alpha^4\Delta^4)\right) \quad (147)$$

□

References

- Bakka, H., Rue, H., Fuglstad, G.-A., Riebler, A., Bolin, D., Illian, J., Krainski, E., Simpson, D., and Lindgren, F. (2018). Spatial modeling with r-inla: A review. *Wiley Interdisciplinary Reviews: Computational Statistics*, 10(6):e1443.
- Besag, J. (1981). On a system of two-dimensional recurrence equations. *Journal of the Royal Statistical Society: Series B (Methodological)*, 43(3):302–309.
- Fuglstad, G.-A., Lindgren, F., Simpson, D., and Rue, H. (2015). Exploring a new class of non-stationary spatial Gaussian random fields with varying local anisotropy. *Statistica Sinica*, pages 115–133.
- Guinness, J. (2018). Permutation and grouping methods for sharpening gaussian process approximations. *Technometrics*, 60(4):415–429.
- Guinness, J. and Fuentes, M. (2017). Circulant embedding of approximate covariances for inference from gaussian data on large lattices. *Journal of computational and Graphical Statistics*, 26(1):88–97.
- Guttorp, P. and Gneiting, T. (2006). Studies in the history of probability and statistics xlix on the matern correlation family. *Biometrika*, 93(4):989–995.
- Higdon, D. (1998). A process-convolution approach to modelling temperatures in the north atlantic ocean. *Environmental and Ecological Statistics*, 5(2):173–190.
- Lindgren, F., Rue, H., and Lindström, J. (2011). An explicit link between Gaussian fields and Gaussian Markov random fields: the stochastic partial differential equation approach. *Journal of the Royal Statistical Society: Series B (Statistical Methodology)*, 73(4):423–498.
- Stein, M. L. (1999). *Interpolation of spatial data: some theory for kriging*. Springer.
- Vecchia, A. V. (1988). Estimation and model identification for continuous spatial processes. *Journal of the Royal Statistical Society: Series B (Methodological)*, 50(2):297–312.
- Whittle, P. (1954). On stationary processes in the plane. *Biometrika*, pages 434–449.
- Whittle, P. (1963). Stochastic processes in several dimensions. *Bulletin of the International Statistical Institute*, 40(2):974–994.

Zhang, H. (2004). Inconsistent estimation and asymptotically equal interpolations in model-based geostatistics. *Journal of the American Statistical Association*, 99(465):250–261.